Quantifying and Enhancing Robustness in Steel Structures: Part 2—Floor Framing Systems

CHRISTOPHER M. FOLEY, KRISTINE BARNES and CARL SCHNEEMAN

Typical structural steel framing systems contain many attributes desired when seeking inherent structural integrity and robustness. The framing systems are most often orthogonal, alleviating the need to layout tying systems and contain many potential secondary load paths (e.g., membrane/catenary action in the steel-concrete composite slab and infill beams). If a better understanding of the demands placed on primary and secondary load paths in the structural steel framing system during abnormal loading events and their likely capacities existed, general structural integrity provisions for structural steel systems could be generated and the tendency for disproportionate collapse in these systems would be better understood.

A companion paper (Foley, Schneeman and Barnes, 2008) provides a detailed review and synthesis of the literature related to design and analysis for progressive collapse resistance and outlines the motivation for the present effort. It discusses the results of a three-dimensional (3D) simulation of 3-, 10- and 20-story buildings exposed to compromised column scenarios and provides insights into the inherent robustness and structural integrity of moment-resisting frames. However, the analyses carried out in this former effort did not consider what may happen at locations within the steel skeleton outside the perimeter at the ground floor level, and it did not attempt to quantify inherent structural integrity contributed by components other than the steel skeleton. Furthermore, the analytical models did not support response simulation considering ineffective interior columns, interior girders, exterior girders, or in-fill beams. If robustness in the structural steel framing system is to be quantified and mechanisms for enhancement identified, analysis must go beyond the simple removal of columns around the perimeter of the framework.

The objectives of the present manuscript are (1) provide a targeted review of literature pertaining to catenary and membrane action in the floor slab within the structural steel building system; (2) provide an overview of the methodologies that have been proposed and validated via experimental testing for quantifying the catenary and membrane mechanisms in concrete floor systems; and (3) outline a methodology for quantifying the membrane and catenary capacity in structural steel floor framing systems, and identify high-level provisions for ensuring structural integrity by enhancing the potential for successful activation of catenary and membrane action in the framing system. Through detailed evaluation of the response of the floor framing systems to compromising event scenarios, it is hoped that the present effort can further contribute to the understanding of the load transfer mechanisms inherent in the structural steel building, provide insights into developing analysis and design methodologies and systems to enhance this inherent structural integrity, and provide guidance for developing simple and effective general structural integrity provisions for specifications.

MEMBRANE AND CATENARY ACTION IN SLAB SYSTEMS

Researchers in the field of reinforced concrete design have had a long history of attempting to understand the tensile behavior of structural concrete floor systems and proposing methodologies for quantifying the beneficial effects of catenary and membrane action. Much of the research conducted in this regard (Hawkins and Mitchell, 1979; Mitchell and Cook, 1984) has made its way into ACI 318 (ACI, 2005) provisions for general structural integrity. Investigators studying the response of structural steel systems to fire have also begun to understand and capitalize on the inherent robustness present in steel framing systems contributed by the reinforcement in the concrete floor slab (Allam, Burgess and Plank, 2000; Bailey, White and Moore, 2000; Huang, Burgess and Plank, 2003a, 2003b).

It has long been recognized that flat plate concrete floor systems have the potential to suffer from disproportionate collapse after a rather simplistic event—punching shear failure at interior and exterior columns (Hawkins and Mitchell, 1979; Mitchell and Cook, 1984). Hawkins and Mitchell (1979) provide a very nice description of the development of

Christopher M. Foley is associate professor, department of civil and environmental engineering, Marquette University, Milwaukee, WI.

Kristine Barnes is a structural engineer, AREVA NP, Inc., Naperville, IL.

Carl Schneeman is a structural engineer, Walker Parking Consultants, Minneapolis, MN.

membrane action in a concrete flat-plate floor system. When a concrete floor is loaded to the point of inelastic behavior, there is a tendency for the bottom fibers (assuming loading is from the top) to lengthen, and this fiber lengthening is restrained by the concrete slab at the perimeter of the panel being loaded. In a theoretical sense, the concrete slab will have a load versus vertical deflection response that exhibits snap-through prior to the formation of membrane tension in the system. The hanging net effect cannot take place without significant vertical deformation, and all sections through the floor plate can be subjected to large tensile strains.

The Hawkins and Mitchell (1979) expressions for computing the membrane capacity of concrete floor panels are simple and include a significant amount of engineering feel. More complicated methods for computing membrane capacity of slab systems are available (Park, 1964; Regan, 1975; Park and Gamble, 1980). The fundamental assumption of the proposed methodology is that the deformed membrane between supports follows a circular shape. This makes the mathematics tractable, and errors are relatively small when compared to the more correct catenary parabola. The basic slab system and membrane forces considered are schematically shown in Figure 1. Two slab span directions are assumed: a short direction, l_1, and a long direction, l_2. The reinforcement area on a per unit length basis in the short and long directions are A_{s1} and A_{s2}, respectively. The normal strains in the fibers of the membrane are assumed to be uniform over the membrane thickness and are functions of the curvature. Uniformly distributed loading over the surface of the membrane is assumed, and positive loading is taken to be downward. Membrane tension forces (edge tensions) per unit length parallel to the short and long directions and tangent to the deformed membrane's mid-surface are T_1 and T_2, respectively.

The free-body diagram for catenary behavior is shown in Figure 2. The tension force in the membrane follows a tangent to the deformed shape at any point along the catenary. There is a tension force resultant at the edge, T_{max}, and the centerline, T, when the uniformly distributed loading, w_o, is applied. A major structural engineering-related issue that needs to be considered when examining catenary and membrane behavior in floor systems is the trade-off between allowing significant catenary deflection, h, and the peak tension force. The catenary forces will significantly increase if the shape of the catenary is held close to the horizontal plane (e.g., a tight-rope). If one does not allow significant deflection in the catenary to occur, tension forces can become very large, thus rendering catenary action infeasible. If one allows significant deflection in the catenary and the strains in any deflected shape assumed will not exceed those corresponding to rupture, these tensile forces can be reduced.

Attention can now be turned to membrane action in the concrete slab portion of the system illustrated in Figure 1. A typical structural mechanics solution procedure (e.g., imposition of vertical equilibrium, ensuring compatibility of deformations, and adherence to constitutive laws for the material) is employed to develop a relationship for the capacity of the tensile membrane that is a function of the edge tension, strain in the membrane (and therefore, vertical deflection), and the panel dimensions. When the panel dimensions differ (e.g., rectangular panel) the membrane capacity of the panel based upon the tensile reinforcement capacity at the edges can be written as (Hawkins and Mitchell, 1979),

$$w_{mem} = \frac{2T_1 \sin\left(\sqrt{6\varepsilon_1}\right)}{l_1} + \frac{2T_2 \sin\left(\frac{l_1}{l_2}\sqrt{6\varepsilon_1}\right)}{l_2} \qquad (1)$$

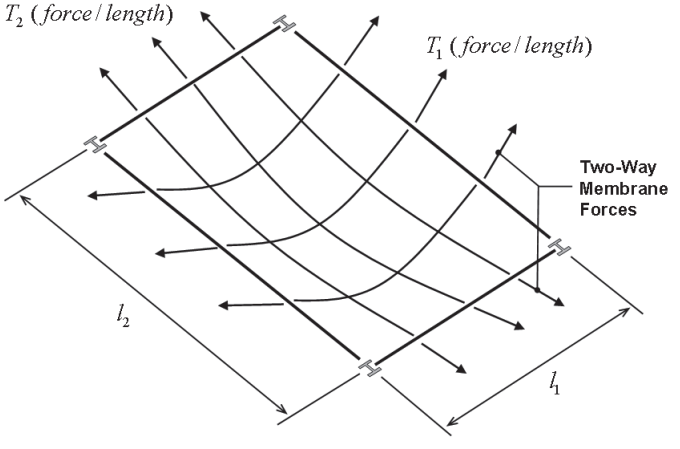

Fig. 1. Two-way membrane action in reinforced concrete slab.

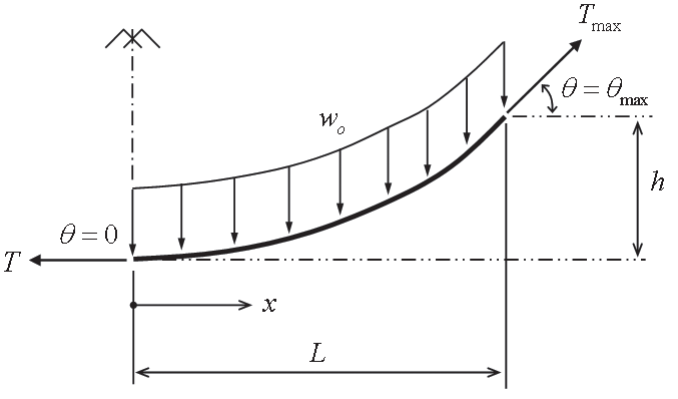

Fig. 2. Fundamental representation of catenary action.

where

ε_1 = tensile strain in the membrane fibers parallel to the short (dominant) direction

As l_2/l_1 increases, the slab panel begins to behave as a single direction membrane. In the present case, welded wire mesh and steel deck are the primary reinforcement components.

The strains in the direction parallel to the short and long dimensions are related to one another as a result of the assumed circular shape of the membrane. The strain in the direction parallel to the short dimension is computed using (Hawkins and Mitchell, 1979),

$$\varepsilon_1 = \varepsilon_2 \left(\frac{l_2}{l_1} \right)^2 \tag{2}$$

Therefore, once the strains in the two directions are computed (long direction assumed, then short direction computed), the constitutive laws for the reinforcement can be used to determine the state of stress and then the tensile membrane forces. The maximum deflection within the panel can be estimated using (Mitchell and Cook, 1984),

$$\delta = \frac{3 l_1 \varepsilon_1}{2 \sin\left(\sqrt{6 \varepsilon_1} \right)} \tag{3}$$

The vertical deflection is important when assessing the capacity of the membrane. Assuming end anchorage is present, the membrane is capable of carrying more loading in a highly deflected configuration for a fixed tensile force capacity. Therefore, if a large amount of loading is present and there is a fixed tensile capacity for the reinforcement in the membrane (assuming no rupturing of the reinforcement), then there is a tendency for the membrane to continue to deflect vertically to generate greater vertical components in the catenary forces.

The response of a slab structure as a membrane depends upon the steel reinforcement, the vertical support conditions, and the horizontal restraint conditions at the panel edges (Mitchell and Cook, 1984). When the slab panel has vertical support at its edges, the slab is capable of providing its own in-plane compression ring restraint conditions at the perimeter. This compression ring helps to resist the horizontal component of the maximum tensile forces (Figure 1). Edge or corner panels can develop the necessary compression ring behavior if the edges are supported by beams that have significant flexural stiffness when compared to the slab itself. Anchorage of the tension reinforcement at the panel edges is also very important to facilitate compression ring formation.

One-way catenary action may also arise in a floor system. A catenary subjected to uniformly distributed loading, w_o, shown in Figure 2, will be utilized as a basis for the following discussion. The uniformly distributed loading capacity of the catenary can be computed using (Hibbeler, 2006),

$$w_o = w_{cat} = \frac{T_{max}}{L} \left[1 + \left(\frac{L}{2h} \right)^2 \right]^{-0.50} \tag{4}$$

The catenary sag is denoted as h, one-half the catenary span is defined as L, and the tension force in the membrane is T at mid-span and T_{max} at the edge. The reinforcement at the central portion and edge of the catenary is assumed to be the same. As the sag increases, the length of the catenary relative to original horizontal span increases, and this can lead to significant strains.

The fundamental theory of the parabolic catenary can be used to develop a relationship for the length along the catenary parabola given by,

$$L' = \int_0^L \left[\sqrt{1 + \frac{4h^2}{L^4} x^2} \right] dx \tag{5}$$

Equation 5 can be used to compute the length of the components in the catenary in its deformed position, and this length can be used along with the initial length to estimate ductility demand in the catenary system.

MEMBRANE ACTION IN COMPOSITE DECK FLOOR SYSTEMS

Although structural steel floor framing systems are significantly different in many ways from that of a two-way flat plate or flat slab cast-in-place concrete system, there are enough similarities to justify using the existing theory and expressions (Hawkins and Mitchell, 1979; Mitchell and Cook, 1984) to assess the inherent integrity and robustness of structural steel floor framing systems.

It is felt that membrane and catenary action are indeed possible within the structural steel framing systems commonly found in buildings, and fire researchers have long recognized the importance of this load transfer mechanism (Wang and Kodur, 2000). Tension reinforcement present in these systems will need to be quantified and their anchorage discussed prior to detailed examination of ineffective supporting member scenarios. In composite steel-concrete floor systems, there is typically welded-wire mesh and light gage steel deck that can be utilized as tension reinforcement within the slab system should membrane and/or catenary action be needed. However, one must understand the usefulness of these components as reinforcing mechanisms in the slab system before it can be relied upon as sources of membrane and catenary reinforcement.

The light gage steel deck is essentially a unidirectional spanning entity. In the direction parallel to the flutes in the

deck, it is likely to be a very useful form of tension reinforcement for facilitating catenary action. However, in the direction orthogonal to the flutes, the steel deck likely has puddle welds or TEK screws that are unlikely to preserve tensile forces within the deck in this direction. Furthermore, the fluted nature of the deck results in a tension force that has two distinct elevations at the floor deck soffit, making it questionable to rely on the steel deck providing tensile membrane or catenary reinforcement in two directions. The present analysis assumes that the steel deck provides one-way reinforcement within the floor framing system. It should be noted that if the steel deck panels are not continuous over the supporting beam, a supplemental force-transfer mechanism must exist.

The welded-wire fabric present in the floor system is also a source of potential membrane and catenary tension reinforcement. This steel fabric generally has a slightly elevated yield stress when compared to the usual mild-steel reinforcement. Furthermore, the spacing of the wires in the mesh can change with direction. This reinforcement is considered continuous through the panel perimeter with sufficient lap splicing throughout. A typical lap splice requirement for 6×6-W1.4×1.4 plain welded wire fabric in tension is 10 in. for concrete with 4,000 psi, 28-day unconfined compression strength (ACI, 2005).

In the steel building system considered in this study, a panel is defined as having infill beams and/or girders bounding a panel of concrete slab. In most cases, the perimeter of the slab panel will have puddle welds or even steel studs connecting the steel deck to the perimeter beams/girders. Furthermore, these perimeter members will have significantly greater flexural stiffness when compared to that of the slab. The present analysis assumes the slab system can develop compression ring anchorage.

The basic process used to assess and quantify the membrane and catenary action present in the structural steel floor framing system is to use Equations 1 through 3 to describe two-way membrane behavior in the floor framing system and Equations 4 and 5 to describe one-way catenary behavior. The strain demands must be compared to rupture strains. This is done using Equation 2 in the case of two-way behavior and Equation 5 in conjunction with the initial horizontal length for one-way behavior. The following sections proceed with evaluating several ineffective element scenarios and make recommendations regarding the levels of inherent robustness in the floor system, or make recommendations regarding simple measures that can be taken to enhance structural integrity in these systems.

INEFFECTIVE ELEMENT SCENARIOS

The present study considered the following main structural components being rendered ineffective: an interior column, an interior infill beam, a spandrel beam, two adjacent infill beams, and spandrel girder. The 30-ft framing bays of the 3-story and 10-story frameworks considered in the companion effort (Foley, Schneeman and Barnes, 2008) are used as base topologies for this study. Exhaustive detail of the computations outlined in this manuscript can be found in Foley, Martin and Schneeman (2007).

Ineffective Infill Beam(s)

The first scenario considered is shown in Figure 3, and it results in two-way membrane action with panel dimensions equal to 20 ft by 30 ft. A 2VLI22 steel deck provides formwork and tension reinforcement for the concrete slab (5 in. total height composite slab) and 6×6-W1.4×W1.4 shrinkage and temperature reinforcement is present. The steel deck is assumed to provide membrane tension reinforcement parallel to the short direction, and the welded wire fabric is assumed to provide reinforcement in both directions. The reinforcement is assumed to have elastic-perfectly-plastic stress-strain behavior. The yield stress of the welded wire mesh is taken as 65 ksi, and the tension area provided on a unit length basis is 0.00233 in.^{2}/in. (ACI, 1997). The steel deck is assumed to have yield stress equal to 40 ksi, and the cross-sectional area on a unit length basis is 0.03542 in.^{2}/in. (Vulcraft, 2005).

If the full cross-sectional area of the steel deck is at yield, the tension force that can be developed is 1.42 kips/in. If the steel deck panel terminates at a beam or girder, the horizontal component of this potential membrane/catenary force will require anchorage. If anchorage mechanisms (e.g., puddle welds, shear studs) are located at 6 in. on center, an estimate

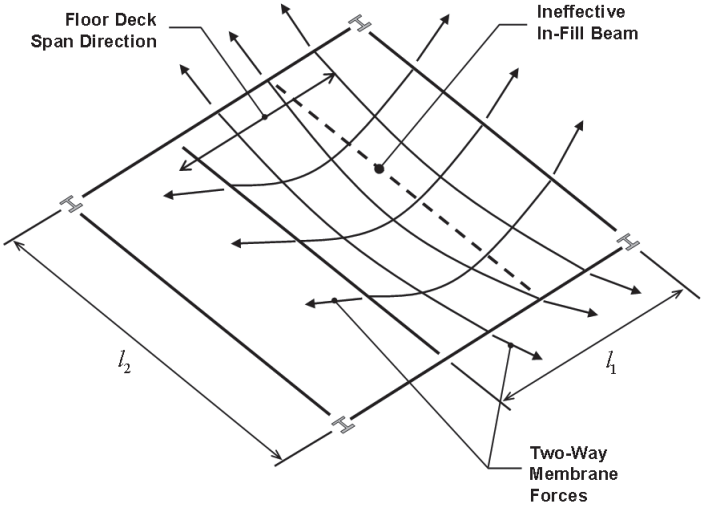

Fig. 3. Schematic of two-way membrane action in composite steel-concrete floor system when one in-fill beam is rendered ineffective.

for the anchorage force is 8,500 lb. The nominal strength of a ⅝-in. arc spot weld to structural steel substrate through 2VLI22 steel deck is 1.64 kips (AISI, 2001). Therefore, ⅝-in. puddle welds at 3 in. on center would yield 550 lb/in. capacity. Therefore, 40% of the steel deck cross-sectional area was assumed to be effective in the analysis. The membrane force in the short direction is composed of a percentage of the total steel deck cross-sectional area at yield and the welded wire mesh (WWM) cross-sectional area at yield. In the long direction, the membrane force is exclusively provided by the cross-sectional area of the WWM at yield.

An analysis of the two-way membrane capacity of the floor slab indicated that the force at the perimeter of the panel in the steel deck was 566 lb/in. and that the force parallel to the long direction was 152 lb/in. The uniformly distributed load-carrying capacity of the panel was estimated to be 110 psf with nearly 7 in. of vertical deflection (Foley et al., 2007). The strain in the reinforcement spanning in the short direction is 0.00225 in./in., which is approximately two times the yield strain for the deck and much less than the yield strain for the WWM. Keeping the yield strain in the steel deck equal to or less than $2\varepsilon_y$ was considered to be sufficient to prevent rupture.

The total loading present on the panel at the instant the infill beam is rendered ineffective is 93 psf (50 psf, concrete steel composite deck; 3 psf, ceiling/floor/fireproofing; 7 psf, m.e.p; 20 psf, partitions; 12.5 psf, live loading). If current progressive collapse mitigation guidelines are employed (GSA, 2003; DOD, 2005), this would require that the two-way membrane be capable of supporting,

$$\beta_{dynam}\left(1.0D + 0.25L\right) = 2\left(93\right) = 186 \text{ psf} > 110 \text{ psf}$$

The membrane is not capable of carrying this loading magnitude; therefore, the system would require additional structural engineering to prevent slab system collapse. If the 2VLI22 gauge deck remains, but mild-steel reinforcement of #3 at 12-in. spacing (60-ksi yield strength) is used, the two-way membrane capacity increases to 189 psf, and a dynamic load factor of 2.0 may be accommodated (Foley et al., 2007). All previous scenarios resulted in membrane deflections of approximately 7 in. and strains in the deck and reinforcement equal to or less than $2\varepsilon_y$.

A second scenario involving two ineffective infill beams is shown in Figure 4. This scenario is interesting because the membrane is square, but the tensile reinforcement is orthotropic. The loading capacity of the 30-ft by 30-ft membrane utilizing 6×6-W1.4×W1.4 welded wire mesh with 2VLI22 steel deck is lower than the previous scenario. The two-way membrane capacity is approximately 93 psf with 12 in. of membrane deflection (Foley et al., 2007). The strain present in the steel deck is approximately $2.2\varepsilon_y$. The benefit of two-way action should be apparent as the capacity of the membrane was reduced 15% from the previous scenario. The typical panel found in structural steel floor systems appears incapable of supporting the required 2.0 multiplier for dynamic effects required by current guidelines (GSA, 2003; DOD, 2005), but is capable of supporting its self-weight and expected point-in-time sustained live loading.

Alternate reinforcement schemes using mild-steel reinforcing bars were also studied (Foley et al., 2007). The yield stress for the mild-steel bars was assumed to be 60 ksi without strain hardening. This study yielded the following reinforcement alternatives:

#3 at 24 in. on center; 0.00458 in.^{2}/in. . . .
119 psf at 12-in. deflection $\left(\beta_{dynam} \simeq 1.3\right)$

#3 at 18 in. on center; 0.00611 in.^{2}/in. . . .
140 psf at 12-in. deflection $\left(\beta_{dynam} \simeq 1.5\right)$

#3 at 12 in. on center; 0.0092 in.^{2}/in. . . . .
178 psf at 12-in. deflection $\left(\beta_{dynam} \simeq 1.9\right)$

Ineffective Spandrel Beam

A scenario involving a spandrel beam being rendered ineffective was also studied (Figure 5). The steel deck flutes run perpendicular to the direction of assumed catenary action. Exterior cladding being supported by the spandrel element is assumed to fall off with the spandrel beam. Welded wire fabric/mesh was found to be incapable of facilitating catenary action in the floor slab (Foley et al., 2007). There are two possibilities for creating structural integrity and robustness in this scenario. The first involves lumping catenary

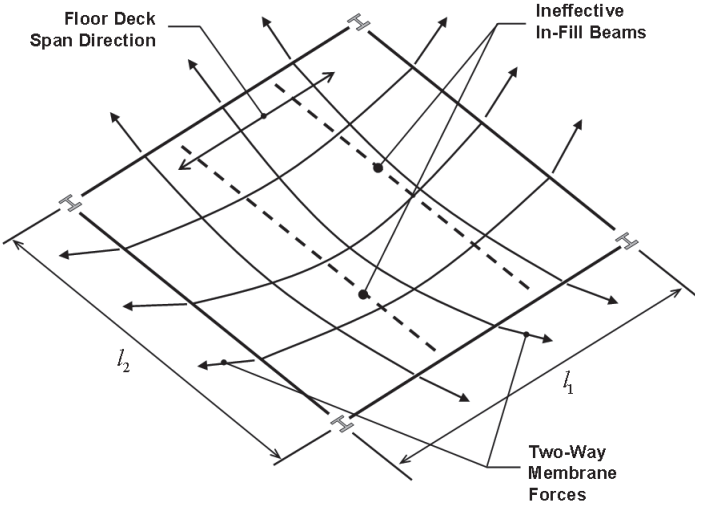

Fig. 4. Schematic of two-way membrane action in composite steel-concrete floor system when two in-fill beams are rendered ineffective.

Table 1. One-Way Catenary Reinforcement Capacities with Variation in Distributed Slab Reinforcement					
Reinforcement Scenario (1)	h, in. (5)	A_s, in.^{2}/ft (2)	q_u, lb/ft^2 (3)	β_{dynam} (4)	$\mu = \frac{\varepsilon_s}{\varepsilon_y}$ (6)
6×6-W1.4×W1.4	16.2	0.028	21.5	0.23	2.4
#3 at 24-in. o.c.	16.2	0.055	39	0.42	2.6
#4 at 18-in. o.c.	16.2	0.133	94	1.01	2.6
#4 at 14-in. o.c.	16.2	0.1714	122	1.31	2.6
#4 at 9-in. o.c.	16.2	0.2667	189	2.03	2.6
#4 at 14-in. o.c.	18.0	0.1714	135	1.45	3.2
#4 at 12-in. o.c.	18.0	0.20	157	1.68	3.2

tensile reinforcement at the perimeter of the slab system (i.e., immediately above the ineffective spandrel in-board of the columns); and the second involves distributing catenary tensile reinforcement. Equations 1 and 4 are used to evaluate the load carrying capacity of the catenary if the yield stress in the reinforcement is attained.

The first scenario considered is lumped mild-steel catenary reinforcement—four #4 Gr. 60 reinforcing bars continuous at the perimeter. The catenary span is 360 in. (30 ft), and the tributary width of deck perpendicular to the catenary is 5 ft. The loading capacity for this scenario was found to be 100 psf (Foley et al., 2007). The strains present in the reinforcement with the assumed catenary sag of 14 in. is approximately $2\varepsilon_y$. One could argue that the 5-ft tributary width is conservative because it is likely that the steel deck could be a very effective cantilever. If the tributary width of slab carried by the catenary drops to 3 ft (assuming that the steel deck and WWM acting together transmit more loading to the first interior in-fill beam), four #4 bars are capable of supporting 168-psf loading, allowing for a dynamic multiplier of 1.8.

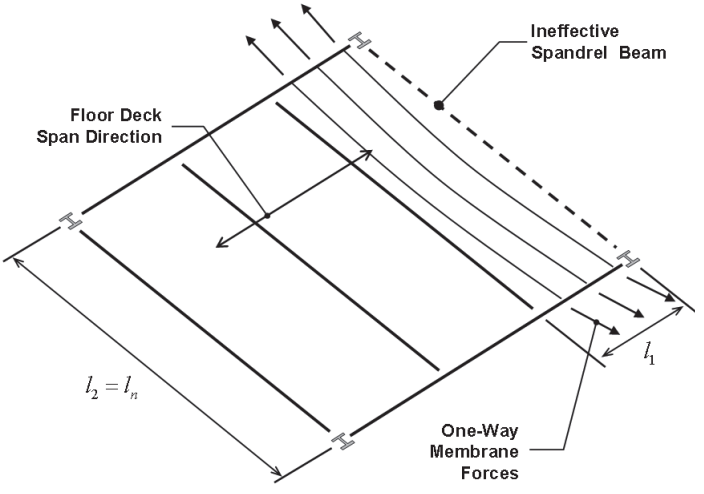

Fig. 5. Schematic illustrating ineffective spandrel beam scenario.

A second mild-steel reinforcement scenario considered reinforcement distributed throughout the slab, thus creating one-way membrane action wherever needed. This creates a tributary width to the catenary of 1 ft. A variety of reinforcement scenarios were considered, and they are shown in Table 1 (Foley et al., 2007). The magnitude of point-in-time static loading present at the time the system is compromised is 93 psf. The reinforcement scenarios and load-carrying capacities indicate that the typical WWM in a steel-concrete composite floor system is not capable of carrying the expected 93-psf loading. It should be noted that more capacity is gained as the catenary is allowed to sag, but one should recognize that with sag comes strain, and the rupture strain may be exceeded.

A second ineffective spandrel beam scenario considered assumes the spandrel beam is lost as well as the first interior infill beam (Figure 6). Two-way action is not considered. Catenary action at the edge of the panel considered in the previous scenario has been deemed ineffective without additional slab reinforcement. The results in Table 1 indicate that if #4 bars are provided at 9 in. on center throughout this bay, a significant level of general structural integrity and enhanced robustness can be gained if the spacing is 18 in. The floor slab with this reinforcement will likely be capable of supporting the expected loading.

Ineffective Spandrel Girder

The final floor member scenario considered is shown in Figure 7. It is assumed that when the spandrel girder is rendered ineffective, exterior cladding attached to this member falls off the structure. This situation benefits from the presence of composite steel deck in the direction of the one-way membrane action. Therefore, this reinforcement is considered in the membrane analysis. It should be noted that because the vertical supporting element at the edge of the panel is lost, two-way action is not considered. It should be emphasized that there is an assumption that the connections at the ends of the beams framing into the exterior columns are capable of supporting the additional loading. The 75% reduction in applied live loading from that used for the original design of the connections makes this assumption palatable.

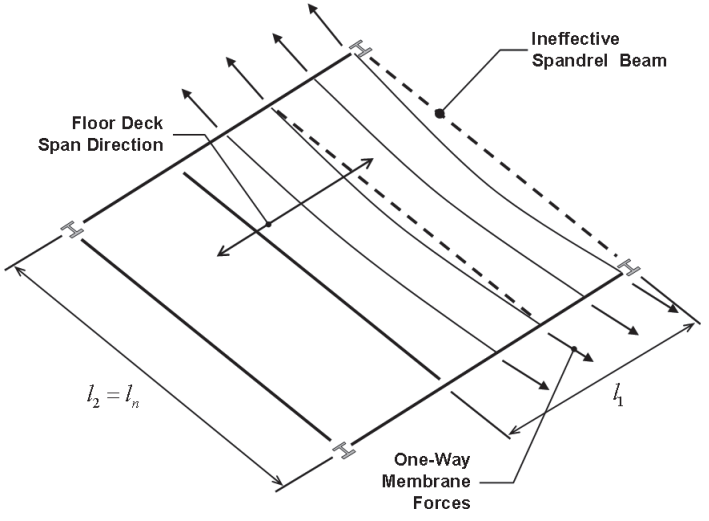

Fig. 6. Schematic illustrating ineffective spandrel and immediately adjacent beam scenario.

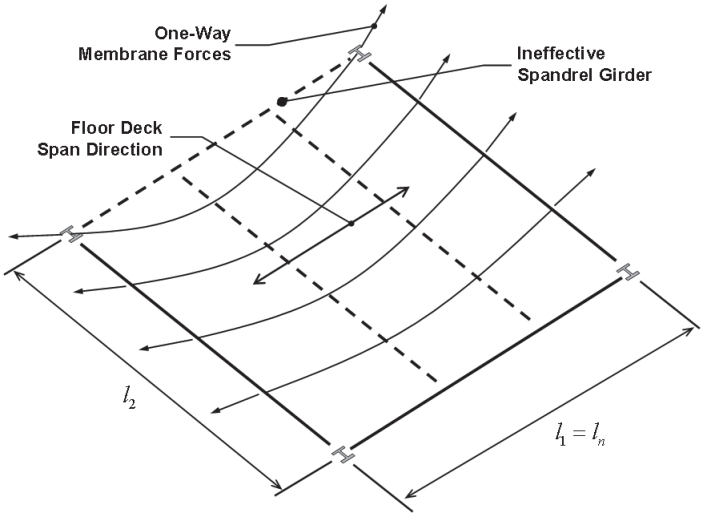

Fig. 7. Schematic illustrating ineffective spandrel girder scenario.

If one assumes that 50% of the steel deck is considered anchored at the end of the catenary and that 2VLI22 composite steel deck is used along with the typical shrinkage and temperature reinforcement (6×6-W1.4×W1.4); the one-way membrane capacity of the system is approximately 102 psf with 13.5 in. of sag and strains in the WWM and steel deck are equal to or less than $2.7\varepsilon_y$ (Foley et al., 2007). Assuming one or both of the panel edges are exterior, the connections at the ends of the catenary must support a tensile force equal to

$$T_{end} = A_{deck} f_{dy} = [0.50(0.03542 \text{ in.}^2/\text{in.})(12 \text{ in./ft})](40 \text{ ksi})$$
$$= 8.5 \text{ kip/ft}$$

Steel studs at 1-ft spacing may be able to develop this force, but it is unknown if the deck is capable of channeling this force to discrete connection points. In the case of continuous panel edges and continuous deck panels over the support, this connection is of moderate concern. The capability of the steel deck and its attachment to the structural steel beam substrate in meeting this demand is worthy of further study.

Ineffective Interior Column

The 3-, 10-, and 20-story building analyses considered in the companion paper (Foley et al., 2008) indicated that as one rises through a steel building framework and loses the beneficial effects of deep beam action in the stories above an ineffective column and the flexural mechanisms provided by several girder lines above the compromised column, the floor system may be required to develop catenary and/or membrane action in addition to flexural capacity in order to resist disproportionate collapse.

The robustness inherent in structural steel simply connected framing systems was evaluated through consideration of the typical interior framing bays present in the 3-story and 10-story buildings previously considered (Foley et al., 2008) and the assumption that an interior column would become ineffective. In this situation, the ineffective column facilitates activation of two-way membrane action in the concrete floor framing system and two-way flexure/catenary action in the structural steel framing. A critical assumption is that each floor carries its own expected point-in-time superimposed loading and self weight. As a result, each floor can be treated as an independent entity within the multistory system. A second important assumption is that the columns at the corners of the panel are not overloaded as the interior column loses its axial capacity. As discussed earlier, the 75%

reduction in live loading from that used in design makes this reasonable.

There is a synergy between the slab and steel grillage that has recently been studied in relation to fire (Allam et al., 2000; Bailey, et al, 2000; Huang, Burgess and Plank, 2000a, 2000b; Burgess, Huang and Plank, 2001; Cai, Burgess and Plank, 2002; Huang, Burgess and Plank, 2003a, 2003b). In the present analysis, a deformation compatibility approach is used in conjunction with two separate static analyses: the first considers two-way membrane action in the slab, and the second considers two-way-grillage catenary/flexure action in the steel framing. These two analysis components are illustrated in Figures 8 and 9. As the interior column is rendered ineffective, the slab and grillage of steel members is forced to deform in a compatible manner, and they both resist vertical deformation to the extent that their strength and stiffness allow. The two-way membrane behavior in the slab is assumed to follow the theory described and used previously. Two way grillage (catenary/flexure) behavior in the steel framing can be computed using nonlinear structural analysis theory. These can be used together to evaluate the robustness present in the typical 30-ft by 30-ft simple structural steel framing system.

The analysis undertaken implies superposition, which may appear to be an incorrect assumption. However, closer examination of system behavior coupled with the assumption that the floor slab is not composite with the steel framing at the strength limit state makes this assumption appropriate for the modeling conducted. As an example, consider two steel plates lying on top of one another. The top plate has a thickness of ½ in. and the bottom plate has a thickness of 1 in. The widths of the plates are identical, their materials have identical stress-strain behavior, and the plates are simply supported with concentrated loading applied at midspan. As the concentrated loading is applied, the plates will attract force according to their flexural stiffness. As expected, the thicker plate will carry a larger percentage of the loading prior to yield. As loading increases, the thicker plate will begin to yield, and its flexural strength will begin to reach a limit. The stiffness of this thicker plate also now reduces as a result of yielding. As yielding in the thicker plate occurs with the corresponding stiffness change, the thinner plate begins to pick up loading and tries its best to compensate for the limited capacity of the thicker plate. In the end, both plates will experience flexural mechanism, and the capacity of the two-plate system is the capacity of the two independent plates added together. Compatibility of deformation must be ensured.

The framing connection considered is a double-angle web connection (i.e., web cleats), and the moment, tension and shear capacities of this connection need to be determined. This process can be started by decomposing the web cleat connection into bolt elements (Figure 10). Researchers have been studying methodologies for determining moment and tension capacities of bolted angle connections for some time (Wales and Rossow, 1983; Astaneh-Asl, Call and McMullin, 1989a; Astaneh-Asl, Nader and Malik, 1989b; DeStefano and Astaneh-Asl, 1991; DeStefano, Astaneh-Asl, DeLuca and Ho, 1991; DeStefano, DeLuca and Astaneh-Asl, 1994; Shen and Astaneh-Asl, 1999; Liu and Astaneh-Asl, 2000a,

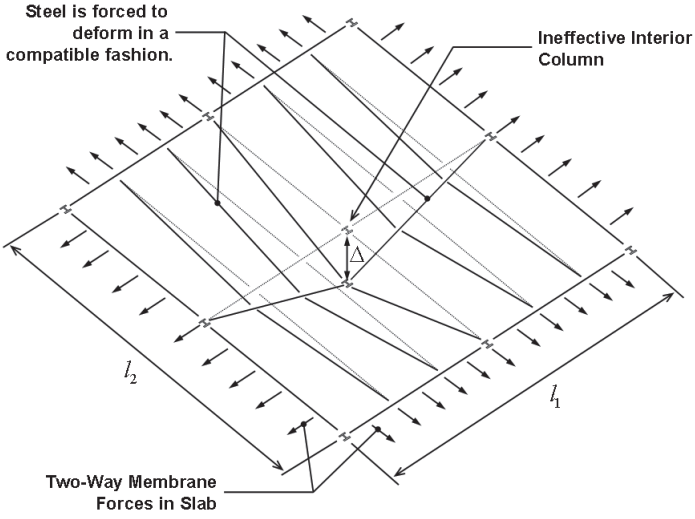

Fig. 8. Two-way membrane action resulting from ineffective interior column.

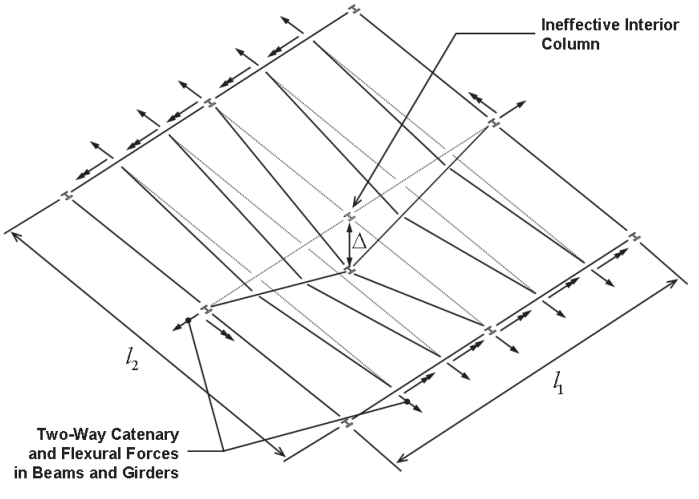

Fig. 9. Two-way catenary/flexure action resulting from ineffective interior column.

2000b; Shen and Astaneh-Asl, 2000; Astaneh-Asl, Liu and McMullin, 2002). The present study uses the approach of Shen and Astaneh-Asl (2000) and Liu and Astaneh-Asl (2000b) to develop nonlinear tension and compression behavior for bolt elements. These bolt elements can then be assembled to form web cleats whereupon moment-rotation behavior of the connections or tension/compression response of the connection can be approximated.

The process begins with developing tension-deflection and compression-deflection response of the double-angle bolt elements (Foley et al., 2007). A tri-linear tension-deformation response for the bolt element is derived using established procedures (Shen and Astaneh-Asl, 1999; Liu and Astaneh-Asl, 2000a, 2000b; Shen and Astaneh-Asl, 2000) with slight modification. The tri-linear bolt element response assumed is shown in Figure 11. Three characteristic points on the response are generated. Point (δ_{T1}, P_{T1}) is defined using the yield moment in the legs of the angle. The initial stiffness, K_{T1}, is the linear elastic stiffness of the bolt element considering bending of the legs perpendicular to the beam web and the axial extension of the leg parallel to the beam web. Point (δ_{T1}, P_{T1}) corresponds to the plastic mechanism capacity of the angle legs perpendicular to the beam web. The post-yield mechanism stiffness is defined as K_{T2}. The final point on the tension-deformation response is (δ_{TU}, P_{TU}), and it corresponds to the ultimate loading for the bolt element exclusive of bolt tension rupture or bolt shear rupture. It is defined through consideration of the angle legs perpendicular to the beam web forming catenary tension between the bolts and the legs parallel to the beam web. The tension in the angle-leg catenary at this ultimate loading is taken to be the loading corresponding to fracture on the net area through the angle leg perpendicular to the beam web. The final stiffness in the response is defined as K_{T3}.

The catenary tension force may or may not be able to form. For example, the bolts may fracture in tension prior to attaining the catenary tension limit state. Therefore, a third point (δ_{T3}, P_{T3}) is used, where P_{T3} is defined through consideration of the following bolt-element limit states (Foley et al., 2007):

- catenary tension fracture in the angle legs perpendicular to the beam web
- tear-out bearing failure of the bolts in the beam web
- tear-out bearing failure of the bolts in the angles
- tension fracture of the bolts including prying action (Thornton, 1985)
- tension fracture of the bolts excluding prying (superfluous)
- shear fracture of the bolts

The third and final point is located along the response defined using K_{T3}. This stiffness, along with P_{T3} defines the deformation capacity of the bolt element, δ_{T3}.

The bolt element compression-deformation response is assumed to be bilinear as indicated in Figure 12. The yield point (δ_{C1}, P_{C1}) is defined by considering three strength limit states (Foley et al., 2007):

- yield in the angle legs parallel to the beam web
- yielding in the beam web
- shear fracture of the bolts

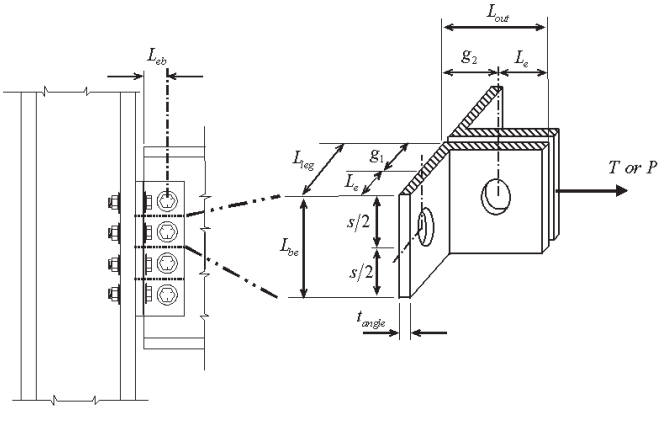

Fig. 10. Web-cleat to bolt element transformation.

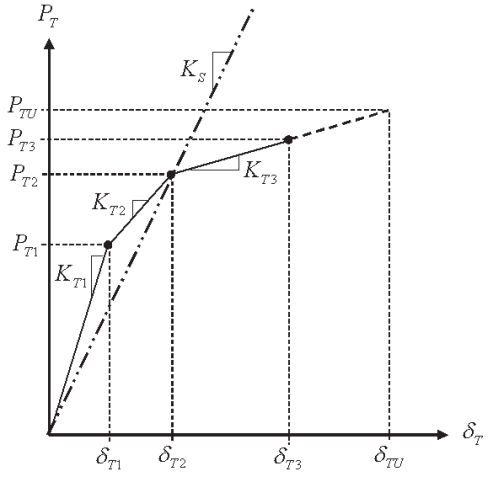

Fig. 11. Double-angle bolt element tension-deformation response.

The ultimate loading capacity of the bolt element in compression is defined through consideration of the following strength limit states (Foley et al., 2007):

- crushing in the angle legs denoted by the ultimate stress being reached in the angle legs parallel to the beam web (conservative)
- crushing in the beam web denoted by the ultimate stress in the beam web being reached (conservative)
- 20% increase above the ultimate bolt shear stress magnitude

The initial stiffness, K_{C1}, is defined using the smaller of two stiffness magnitudes. If beam web yielding controls, the stiffness is defined as,

$$K_{C1} = \frac{A_{web}E}{L_c} \tag{6}$$

and if angle leg yielding controls, the stiffness is defined by,

$$K_{C1} = \frac{A_{angles}E}{L_c} \tag{7}$$

The areas are defined on the basis of the bolt element dimension, L_{be}. The compression length in the angle (or length over which strain accumulates in the beam web) is defined as,

$$L_c = g_2 - \frac{d_h}{2} \tag{8}$$

The post-yield stiffness is defined rather arbitrarily using a 0.5% multiplier to account for moderate strain hardening in the material on the way to crushing. It should be noted that the behavior of the supporting element (e.g., a column flange, a column web, and girder web) is omitted. This is likely very important, but the complexity incurred through consideration of this behavior would render the analysis proposed intractable. Obviously, this requires further evaluation.

Nonlinear tension and compression response for a bolt element consisting of A325-N bolts in 2L4×3.5 were computed (Foley et al., 2007). Expected yield and ultimate tensile stresses for the materials were used. The tension- and compression-deformation response parameters for bolt elements consisting of various angle leg thicknesses are given in Table 2. These parameters depend upon the limits states discussed previously; therefore, the beam web thickness will affect the parameter magnitudes. The W-shapes assumed are consistent with those in the buildings analyzed previously. The tension and compression response for the bolt elements are shown in Figures 13 and 14. The tension-deformation response varies considerably with beam shape and angle thickness. When thin angles are considered, the catenary tension action is allowed to form and rupture of the angle legs is the controlling limit state. However, as the angles get thicker, other limit states control the behavior. This is indicated by the "capping" of the tension forces in the 5⁄16-, 3⁄8- and 1⁄2-in. angle thickness in the W18×35 beam shape and the 3⁄8- and 1⁄2-in. angle thickness with the W21×68 girder shape. The compression-deformation response indicates that the limit states controlling the strength are consistent.

The bolt element ultimate strengths can be used to contribute to the determination of the tension capacity of the double-angle connections through simple summation of

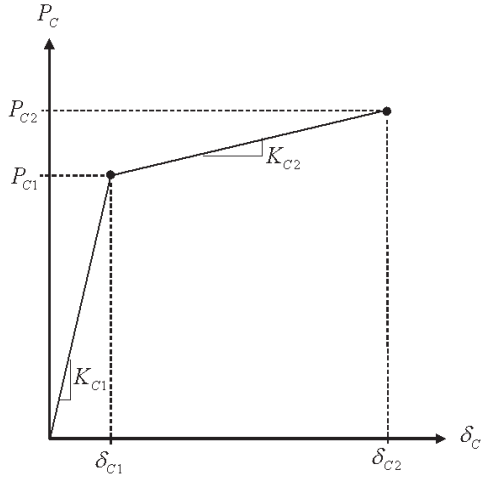

Fig. 12. Double-angle bolt element compression-deformation response.

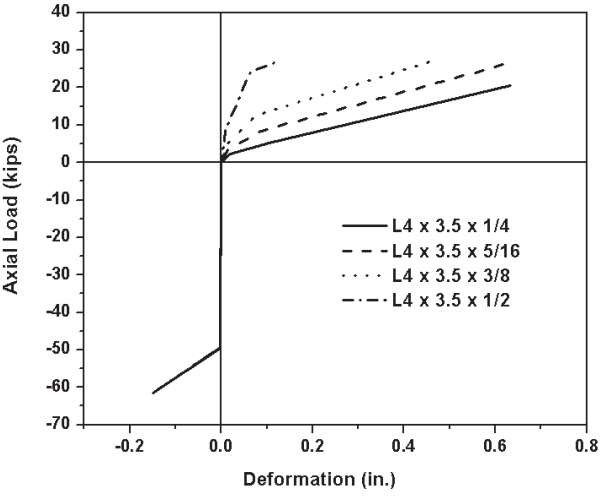

Fig. 13. Bolt element tension and compression response for L4×3.5 double angles and W18×35.

Table 2. Bolt-Element Tension and Compression Response Parameters for Varying Angle Thickness									
Response Direction (1)	Parameter (2)	W18×35				W21×68			
		L4×3½ Angles				L4×3½ Angles			
		¼ (3)	5/16 (4)	⅜ (5)	½ (6)	¼ (7)	5/16 (8)	⅜ (9)	½ (10)
Tension	δ_{T1}, in.	0.019	0.015	0.013	0.0095	0.019	0.015	0.013	0.0095
	δ_{T2}, in.	0.105	0.088	0.077	0.064	0.105	0.088	0.077	0.064
	δ_{T3}, in.	0.632	0.640	0.457	0.124	0.632	0.697	0.752	0.386
	P_{T1}, kips	2.205	3.445	4.961	8.820	2.205	3.445	4.961	8.820
	P_{T2}, kips	5.232	8.462	12.629	24.212	5.232	8.462	12.629	24.212
	P_{T3}, kips	20.491	26.873	26.873	26.873	20.491	28.745	37.93	38.519
	K_{T1}, kips/in.	116.00	226.56	391.50	928.00	116.00	226.56	391.50	928.00
	K_{T2}, kips/in.	35.344	69.031	119.28	282.75	35.344	69.031	119.28	282.75
	K_{T3}, kips/in.	28.947	33.326	37.480	44.489	28.947	33.326	37.480	44.489
Compression	δ_{C1}, in.	0.0030	0.0030	0.0030	0.0030	0.0022	0.0022	0.0022	0.0022
	δ_{C2}, in.	0.1490	0.149	0.149	0.149	0.092	0.092	0.092	0.092
	P_{C1}, kips	49.500	49.500	49.500	49.500	52.590	52.590	52.590	52.590
	P_{C2}, kips	61.425	61.425	61.425	61.425	63.108	63.108	63.108	63.108
	K_{C1}, kips/in.	16380	16380	16380	16380	23470	23470	23470	23470
	K_{C2}, kips/in.	81.882	81.882	81.882	81.882	117.36	117.36	117.36	117.36

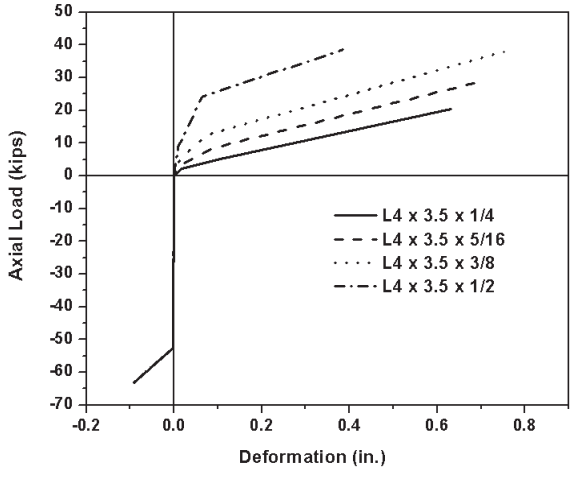

Fig. 14. Bolt element tension and compression response for L4×3.5 double angles and W21×68.

the bolt element tension strengths. However, two additional strength limits states must be considered beyond those considered in the bolt element strength determination. Therefore, the tensile capacity of the double-angle connection is determined through consideration of the following limit states (Foley et al., 2007):

- shear rupture of the bolts
- tension fracture of the bolts, including prying
- block shear rupture in the angle legs parallel to the beam web
- block shear rupture in the beam web
- bearing tear out failure in the angle legs parallel to the beam web
- bearing tear out failure in the beam web
- catenary tension-rupture in the angle legs perpendicular to the beam web

The pure moment capacity of the double-angle web connection is determined using the bolt element tension- and compression-deformation response parameters described previously (Table 2). The pure moment condition is defined by the deformation and force states shown in Figure 15. The process for determining the pure moment capacity of the connection begins with defining the tension and compression response for each bolt element in the connection (Foley et al., 2007). A controlling state of deformation in the extreme tension angle, δ_4, or extreme compression angle, δ_1, is assumed. These deformations are taken from the curves corresponding to the angles in the bolt element. The connection rotation angle, θ, is then varied until the summation of all forces determined using the bolt element response curves is zero. This corresponds to the pure moment capacity of the double-angle connection. It should be noted that this process is iterative and the compression or tension deformation limit states control the behavior.

The shear strength of the double-angle connection given the beam shape chosen can be determined using the AISC *Load and Resistance Factor Design Manual of Steel Construction* (AISC, 2001), hereafter referred to as the AISC *Manual*. It should be noted that allowable stress design load combinations were utilized and therefore, all manual-obtained strengths were divided by 0.75. The shear strengths for the double angles and beam shapes considered assume L_{ev} = 1.5 in., L_{eh} = 1.5 in., ϕ = 1.0, and ¾-in. A325-N bolts in standard holes.

The beams in the grillage are assumed to be W18×35, and the girders are W21×68. The W18 sections can support three to five bolt rows, while the W21 sections can support four to six bolt rows with traditional spacing and end distances (AISC, 2001). Therefore, only these numbers of bolt rows were considered. Table 3 illustrates the pure tension, pure shear, and pure moment capacities of the double angle connections considered (Foley et al., 2007). All shear strengths are controlled by the strength of the beam or girder web (with yield stress of 50 ksi). A † symbol denotes exceptions where the shear strength is limited by the connection angle and/or bolt strength.

Table 3 indicates that the double-angle connection alone has a tensile capacity that ranges from 0.08 to 0.26 of the yield load of the beam cross-section. These are fairly significant tensile capacities (if taken as cumulative over all beam and girder members within the 3D system). The loading capacities are consistent with those found through testing (Owens and Moore, 1992). The moment capacities are very low, however. The bending moment capacities range from 0.05 to 0.18 of the plastic moment capacity of the beam cross-section. This is consistent with the strength portion of the definition of flexible connections (AISC, 2005).

Bilinear moment-rotation response and axial load-extension response curves can be generated for the double-angle connections using the bolt element models. The connections in the grillage are not expected to go into compression in the ineffective column scenario considered. The tension secant stiffness for the bolt element can be defined as shown in Figure 11 (Foley et al., 2007);

$$k_{BE} = K_s = \frac{P_{T2}}{\delta_{T2}} \tag{9}$$

The tensile capacity of each bolt element in the double-angle connection contributes to the tensile and moment capacity of the connection. The bilinear tension-deformation response of each bolt element is characterized by the secant stiffness, k_{BE}, and the bolt element tensile capacity, P_{T3}.

The rotational and axial stiffness of the web-cleat connections are estimated using the magnitudes of the bolt element secant stiffness. The axial stiffness of the double angle connection is the sum of the stiffness of each bolt element in the web cleat,

$$K_\delta = \sum_{i=1}^{n_b} k_{BE,i} \tag{10}$$

The rotational stiffness of the web-cleat connection varies with the number of bolts and a schematic illustration of its computation is shown in Figure 15. If the bolt element stiffness, k_{BE}, is known and there is n_b bolt elements in the web cleat connection, the rotational stiffness can be computed as (Foley et al., 2007),

$$K_\theta = \sum_{i=1}^{n_b-1} i^2 \left(k_{BE} s^2\right) \tag{11}$$

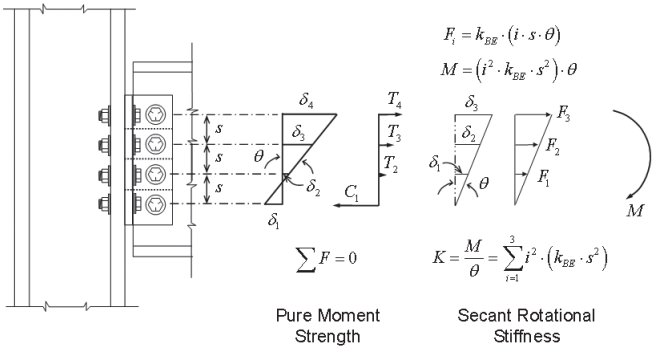

Fig. 15. Schematic illustrating procedure used to compute web-cleat connection flexural strength and stiffness.

Table 3. Pure Tensile, Pure Shear and Pure Moment Capacities for Double Angle Connections							
		W18×35			W21×68		
L4 × 3½ Thickness (1)	Bolt Rows (2)	Axial $\left(\frac{P}{P_y}\right)$ kips (3)	Shear $\left(\frac{V}{V_y}\right)$ kips (4)	Moment $\left(\frac{M}{M_p}\right)$ kip-ft (5)	Axial $\left(\frac{P}{P_y}\right)$ kips (6)	Shear $\left(\frac{V}{V_y}\right)$ kips (7)	Moment $\left(\frac{M}{M_p}\right)$ kip-ft (8)
¼ in.	3	61.5 (0.12)	78.0 (0.31)	13.07 (0.05)	—	—	—
	4	82.0 (0.16)	102.8 (0.41)	24.61 (0.09)	82.0 (0.08)	138.7 † (0.33)	24.61 (0.04)
	5	102.5 (0.20)	127.6 (0.50)	39.03 (0.14)	102.5 (0.10)	176.0 † (0.41)	39.54 (0.06)
	6	—	—	—	123.0 (0.12)	213.3 † (0.50)	56.28 (0.08)
5⁄16 in.	3	80.6 (0.16)	78.0 (0.31)	17.47 (0.06)	—	—	—
	4	107.5 (0.21)	102.8 (0.41)	32.21 (0.12)	115.0 (0.12)	147.3 (0.35)	34.60 (0.05)
	5	134.4 (0.26)	127.6 (0.50)	46.06 (0.17)	143.7 (0.14)	182.9 (0.43)	46.17 (0.07)
	6	—	—	—	172.5 (0.17)	218.4 (0.51)	57.98 (0.09)
⅜ in.	3	80.6 (0.16)	78.0 (0.31)	18.00 (0.06)	—	—	—
	4	107.5 (0.21)	102.8 (0.41)	33.07 (0.12)	151.7 (0.15)	147.3 (0.35)	35.28 (0.05)
	5	134.4 (0.26)	127.6 (0.50)	49.95 (0.18)	189.6 (0.19)	182.9 (0.43)	46.38 (0.07)
	6	—	—	—	227.6 (0.23)	218.4 (0.51)	65.00 (0.10)
½ in.	3	80.6 (0.16)	78.0 (0.31)	19.15 (0.07)	—	—	—
	4	107.5 (0.21)	102.8 (0.41)	32.95 (0.12)	154.1 (0.15)	147.3 (0.35)	37.68 (0.06)
	5	134.4 (0.26)	127.6 (0.50)	50.26 (0.18)	192.6 (0.19)	182.9 (0.43)	61.81 (0.09)
	6	—	—	—	231.1 (0.23)	218.4 (0.51)	93.34 (0.14)

where

s = pitch of the bolt elements (taken as a constant value of 3 in.)

The axial stiffness and flexural stiffness of the web cleat connections can be defined as a function of the axial rigidity and flexural rigidity of the connected member,

$$K_\delta = \alpha_\delta \frac{AE}{L} \tag{12}$$

$$K_\theta = \alpha_\theta \left(\frac{EI}{L}\right) \tag{13}$$

The stiffness characteristics of the steel grillage connections are summarized in Table 4. The rotational stiffness of the web-cleat connections are well below the stiffness limit corresponding to flexible connections (AISC, 2005) given by $\alpha_\theta = 2$. The majority of the rotational stiffness multipliers lie in the range $0.05 \le \alpha_\theta \le 1.50$. One exception is the five-bolt arrangement in the W18×35 beam member. The axial stiffness multiplier for the majority of the connection arrangements lies in the range $0.10 \le \alpha_\theta \le 1.8$ with an exception being the five-bolt connection in the W18×35 member with $\alpha_\delta = 2.3$.

The system analysis begins by computing the capacity of the concrete-steel composite slab system acting as a two-way membrane. The membrane capacity of the concrete slab-steel deck system is approximately 50 psf at 26.2 in. of vertical deflection at the center of the panel (Foley et al., 2007). This magnitude of vertical deflection corresponds to an approximate rotational demand of,

$$\theta = \tan^{-1}\frac{26.1 \text{ in.}}{30 \text{ ft}(12)} = 0.073 \text{ rad}$$

which is below a recommended limit of 0.21 rad (GSA, 2003). It should also be noted that the rotation computed here is total rotation (elastic plus plastic components). The tension force in the steel deck running perpendicular to the in-fill beams is approximately 566 lb/in. (Foley et al., 2007), which is consistent with all previous computations.

A structural analysis model for the steel floor framing system (shown in Figure 16) was developed for use in MASTAN2 (Ziemian and McGuire, 2000). The model contains structural steel beam-column elements, bilinear partially restrained connections, and also axial-load-moment interaction diagrams that are used to define yielding at the ends of the beam-column elements. The basis for the analytical model is a structural steel grillage with fixed supports at all beams and columns located at the perimeter of the 60-ft by 60-ft panel. All members are modeled using multiple elements: ten for infill beams and nine for girders. The infill beams were modeled using four analytical segments. Two segments (half of the beam length) were centered on the beam midspan. The end one-quarter lengths of the beam were subdivided into four additional segments to facilitate connection modeling. Therefore, all infill beams contain end segments that are 1/16 of their span. The end segments in the girders (at column supports and interior column locations) were broken down into four segments resulting in end connection segments 1/12 of the girder span in length.

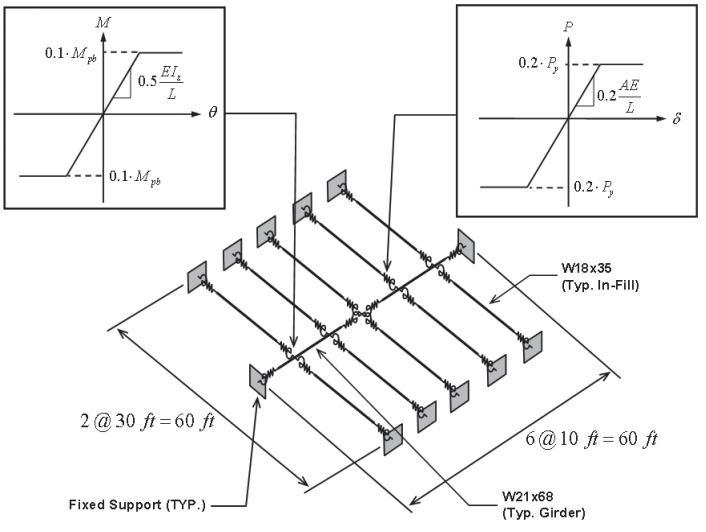

Fig. 16. Steel grillage model schematic (System 1) illustrating axial and moment connection modeling for MASTAN2 nonlinear analysis.

The connection characteristics typical of web-angle connections provided in Tables 3 and 4 were established in MASTAN2 in an indirect manner (Foley et al., 2007). Figure 16 illustrates the bilinear moment-rotation and load-extension behavior assumed in the connections. The axial tension and moment capacities chosen were consistent with those indicated in Table 3. Stiffness of the connections assumed were consistent with those found in Table 4. The bilinear connection characteristics are generated in MASTAN2 by using the built-in partial connection restraint capability for moment and then adjusting member cross-section properties to achieve moment capacities, axial stiffness characteristics, and axial capacity.

The end connections were modeled in the analytical segments of the beams and girders located immediately adjacent to the fixed supports, the supporting girders, and the interior column. The connection rotational stiffness was input using the built-in capabilities with the magnitude indicated in Figure 16 (for the first system considered—System 1). The connection moment capacity was input into the analysis by adjusting the beam or girder's plastic section modulus to $0.1Z_x$. This resulted in a plastic moment capacity in the end regions of the infill beams at the levels indicated in Figure 16. The axial loading characteristics were included in a slightly different manner (MASTAN2 does not allow axial hinges). The cross-sectional areas of the beam or girder in the end connection segments were defined to be 20% of the cross-sectional area of the members outside this hinge region. This reduction in cross-sectional area also created implied linear spring stiffness in this isolated region of the beam equal to 20% of the member's axial rigidity.

The method of modeling connections creates a "stub member" that has an axial capacity that is the same as the intended connection and a moment capacity that is the same as the connection intended. MASTAN2 then uses these pieces of information to create an interaction (yield) surface of

Table 4. Stiffness and Characteristics of Web Cleat Connections								
L4×3½ Thickness and Secant Stiffness Parameters (1)	k_{BE} (kip/in.) (2)	Bolt Rows (3)	K_δ (kip/in.) (4)	K_θ (kip-in./rad) (5)	W18×35 AE/L = 829.7 EI/L = 41,083		W21×68 AE/L = 1,611 EI/L = 119,222	
					α_δ (6)	α_θ (7)	α_δ (8)	α_θ (9)
¼ in. δ_{T2} = 0.105 in. P_{T2} = 5.23 kips	49.81	3	149.43	2,241.5	0.18	0.05	—	—
		4	199.24	6,276.1	0.24	0.15	0.12	0.05
		5	249.05	13,448.7	0.30	0.33	0.15	0.11
		6	298.86	24,656.0	—	—	0.19	0.21
5/16 in. δ_{T2} = 0.088 in. P_{T2} = 8.46 kips	96.14	3	288.42	4,326.3	0.35	0.11	—	—
		4	384.56	12,113.6	0.46	0.29	0.24	0.10
		5	480.70	25,957.8	0.58	0.63	0.30	0.22
		6	576.84	47,589.3	—	—	0.36	0.40
⅜ in. δ_{T2} = 0.077 in. P_{T2} = 12.63 kips	164.03	3	492.09	7,381.4	0.59	0.18	—	—
		4	656.12	20,667.8	0.79	0.50	0.41	0.17
		5	820.15	44,288.1	0.99	1.08	0.51	0.37
		6	984.18	81,194.9	—	—	0.61	0.68
½ in. δ_{T2} = 0.064 in. P_{T2} = 24.21 kips	378.28	3	1,134.8	17,022.6	1.37	0.41	—	—
		4	1,513.1	47,663.3	1.82	1.16	0.94	0.40
		5	1,891.4	102,136	2.28	2.49	1.17	0.86
		6	2,269.7	187,249	—	—	1.41	1.57

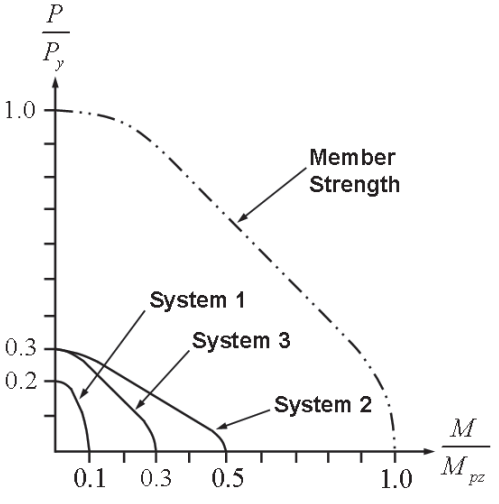

Fig. 17. Member and connection interaction surfaces for connected member and three grillage systems.

the form shown in Figure 17. It should be noted that minor-axis bending is assumed to have a connection capacity that is equal to the minor-axis plastic moment capacity of the members, and the connection stiffness in the minor-axis direction is assumed to be fully restrained. The validity of this interaction diagram for the end connections should be validated with experimental testing.

The beam members in the system were assumed to be composed of 50-ksi steel, and the expected yield stress of the material (55 ksi) was used. The strength ratios given in Table 3 are based upon 50 ksi. Uniformly distributed loading was applied to the in-fill beams in the system. The expected loading used previously was 93 psf. The floor slab system is capable of providing 50 psf toward this total with approximately 26 in. of deformation as discussed earlier. The steel grillage will then be required to carry the following superimposed loading (with a deformation that is assumed to be compatible),

$$q_{grillage} = \beta_{dynam}\left(1.0D + 0.25L\right) - 50$$
$$= \beta_{dynam}\left(93\,\text{psf}\right) - 50\,\text{psf}$$

At pseudo-dynamic loading levels (β_{dynam} = 2.0) prescribed in the GSA Guidelines (GSA, 2003), the grillage will need to support a uniformly distributed loading of 136 psf. Former studies (Marchand and Alfawakhiri, 2004; Liu, Davison and Tyas, 2005; Powell, 2005) and the companion effort (Foley et al., 2008) have shown that the multiplier commonly used to simulate dynamic loading can vary considerably. If the supporting column is simply compromised (i.e., it still has a fraction of its initial load capacity), then one might argue that the self-weight and mean point-in-time sustained live loading needs to be carried without dynamic amplification. In this case, the grillage must support 43-psf superimposed loading. A reference loading of 108 psf was assumed and this corresponds to β_{dynam} = 1.7.

Three systems were considered. Each had varying connection characteristics for the beam-to-girder and girder-to-column connections. System 1 contains the connection strength and stiffness characteristics shown in Figure 16. The load-deformation response is shown in Figure 18, and it indicates that there is a very early transition from flexural behavior to catenary behavior. The connection strengths and stiffness shown in Figure 16 reveal that the cross-sections at the ends of the members reach the yield surfaces very early in the response and the large displacements result in catenary tension in the grillage forming. The applied load ratio that results in deformations compatible with the membrane displacement computed earlier (26 in.) is 0.46, indicating that the capacity of the system (both slab and grillage) is,

$$q_{cap} = 0.46(108) + 50$$

$$\approx 100 \text{ psf}$$

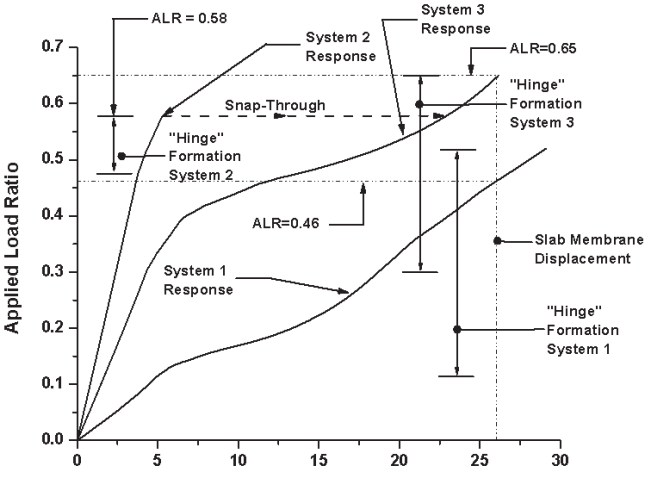

Fig. 18. Load deformation response of three grillage systems considered.

Therefore, the system appears to be capable of supporting its self-weight and the expected point in time sustained live loading with minor reserve for dynamic amplification, β_{dynam} = 100/93 = 1.08.

At 26 in. of vertical displacement, the total rotation over the beam and girder span of 30 ft was approximately 0.07 rad. This is very close to the plastic rotational limit of 0.06 rad recommended for web-angle connections (FEMA, 2000). However, the present rotational demand is "total," and the plastic demand will likely align itself closer to this limit. Therefore, the rotational demands at the level of loading considered are not likely to cause rupture of the connections, but should be further evaluated.

It should be noted that the response estimates were for a system without special modification or design considerations. Inspection of Tables 3 and 4 indicate the following connection configurations yield strength and stiffness characteristics consistent with the analytical assumptions,

W18×35 L4×3½×5⁄16, ⅜, ½ with 4 or 5 bolt rows

W21×68 L4×3½×⅜, ½ with 5 or 6 bolt rows

These angles will yield axial stiffness magnitudes that are a little bit stiffer than the analytical model and bending stiffness magnitudes that are slightly larger as well. The analysis results indicate that in order to enhance structural integrity in the steel system, one is better off choosing connection angles on the upper-end of those provided in the AISC *Manual* (AISC, 2001) and using the maximum number of bolt rows that the beam or girder web can support.

There are other connection types available for use in beam-to-girder and girder-to-column connections. For example, partially restrained beam-to-girder connections have been proposed (Rex and Easterling, 2002), and there is long-standing use of partially restrained girder-to-column connections. A second model was analyzed, and the connections chosen in this case were stronger and stiffer with respect to bending, but had slightly more strength and stiffness with respect to axial deformations. This simulates the concrete slab contributing to increased flexural stiffness and strength. This system (System 2) has the following connection characteristics,

$$P \approx 0.3P_y \text{ and } K_\delta \approx 0.3\frac{AE}{L} \qquad M \approx 0.3M_p \text{ and } K_\theta \approx 5\frac{EI}{L}$$

The connection rotational stiffness and strength are close to those previously reported for partially restrained beam-to-girder connections (Rex and Easterling, 2002). The axial strength and stiffness were increased slightly from that of System 1 to simulate the addition of a seat angle.

The same reference loading of 108 psf was applied to the steel grillage with the understanding that membrane

action in the slab would support 50 psf. The load deformation response of System 2 is shown in Figure 18. The vertical deformation corresponding to the steel grillage strength is insufficient to activate catenary action, and a conversion to catenary action will be needed once the flexural plastic hinge mechanism forms (e.g., snap-through type behavior). However, the structural analysis is not able to consider this transformation because the tangent stiffness matrix is singular at the instant these beam mechanisms form. There appears to be a better synergy in response between the slab system and the structural steel grillage in System 1. The benefits of this type of response remain to be fully quantified and understood.

The experimental rotations attained by Rex and Easterling (2002) for the partially restrained beam-to-girder connections were on the order of 0.05 rad. If one were to rely on catenary action after the flexural mechanisms occur, the vertical deformations in the system would likely rapidly increase to those found in the first system (approximately 26 in.). As a result, the rotational demands on these connections are likely to be on the order of 0.07 rad. It is unclear if the partially-restrained beam-to-girder connection can support this level of rotational demand without fracture, and additional study is recommended.

A third system evaluated had a better balance between axial capacity and moment capacity than System 2 and had the following connection characteristics;

$$P \approx 0.3P_y \text{ and } K_\delta \approx 0.3\frac{AE}{L} \qquad M \approx 0.3M_p \text{ and } K_\theta \approx 2\frac{EI}{L}$$

The load deformation response of this system is given in Figure 18, and it exhibits a smooth transition between flexural mechanism formation and catenary action. As in System 1, there is a significant range of loading over which the interaction surface at the member ends is reached. The increased flexural stiffness in the connections when compared to System 1 is the reason for the lessened vertical deformation prior to the formation of catenary tension behavior in the grillage.

The analysis outlined indicates that when connection moment capacity is low, there is a smooth transition between the initial formation of the flexural mechanism and the secondary catenary tension load transfer mechanism. If the moment capacity is too large, a significant magnitude of vertical displacement may rapidly take place prior to catenary formation. This appears undesirable, and further study is warranted. It is interesting to note that the desired behavior can likely be achieved in the structural steel framing systems considered; therefore, this study suggests the potential for limited special consideration of interior column ineffectiveness if the web angle bolt row recommendations previously described are followed.

CONCLUDING REMARKS

A variety of compromising scenarios in a typical steel floor framing system were considered in which interior infill beams, spandrel beams, and interior columns were rendered ineffective. The base system included 2VLI22 steel deck (5 in. total height composite slab) and 6×6-W1.4×W1.4 welded wire mesh reinforcement. Conclusions regarding behavior and strength of the typical slab system under a variety of compromising events follow.

The slab system typically present in a structural steel building appears capable of carrying point-in-time loading in the event infill beams are rendered ineffective. This statement quantifies one measure of the inherent structural integrity or robustness in the system. The membrane action in the slab system is most effectively enhanced by adding the mild steel reinforcement. The most effective method to enhance robustness and meet GSA-level dynamic multipliers in the event a spandrel beam is lost was determined to be providing a band of mild-steel reinforcement at the perimeter of the slab system. Distribution of mild-steel slab reinforcement throughout the exterior bays in the steel system appears to be an economical way to enhance inherent structural integrity in the case of spandrel beam loss coupled with the loss of adjacent infill beams. Another situation considered was the loss of a spandrel girder. The typical slab arrangement considered was shown to be capable of carrying point-in-time loading after such an event, thereby demonstrating the system has inherent robustness. Enhancing this is most economically attained through additional slab reinforcement.

A scenario whereby an interior column is rendered ineffective was also considered. A static nonlinear analysis of the typical 30-ft by 30-ft framing system that included nonlinear connection behavior consistent with that of web-cleat connections was conducted. The analysis indicated that the compromised system will likely be able to support the self-weight, partitions, and expected point-in-time sustained live loading of the floor system. It should be noted that dynamic response of the system needs to be evaluated in order to fully appreciate the demands that will be placed on puddle welds, shear studs, and internal slab reinforcement. The analysis results indicate that in order to improve the inherent structural integrity in the steel system, one should select connection angle thicknesses on the upper-end of those provided in the AISC *Manual* (AISC, 2001). It is also recommended to use the maximum number of bolt rows that the beam or girder web can support. Both of these rather simplistic measures will enhance the inherent robustness in the system.

The analysis conducted also indicated that it is likely more beneficial to have smaller moment capacity and flexural stiffness for connections distributed throughout the floor framing system (typically present in typical structural steel framing). When the moment capacity is low, there is the opportunity for smooth transition between the formation of the flexural

mechanism and the catenary tension behavior after the initial flexural mechanism forms. If the moment capacity is too large, there may be snap-through-type behavior, whereupon a significant magnitude of vertical displacement will rapidly take place prior to catenary mechanism formation. This appears undesirable, and further study is warranted.

In general, the analysis conducted indicates that balance between membrane action in the slab and catenary action in the steel grillage can be attained when the following axial and moment characteristics are met in regard to the connections at the ends of the beams and girders in the structural steel system:

$$M_{conn} \leq 0.30 M_{pb} \text{ and } K_{\theta} \leq 2\frac{EI}{L}$$

$$P_{conn} \leq 0.3 P_{y} \text{ and } K_{\delta} \leq 0.3\frac{AE}{L}$$

Therefore, this study suggests that there is opportunity to avoid special structural engineering consideration of interior column ineffectiveness scenarios if the web angle bolt row recommendations previously described are followed and larger connection angle thicknesses are implemented.

It is recommended that the response of the entire 3D steel building with the connection characteristics outlined in this section be conducted. This will likely lead to some very interesting results with regard to the true robustness inherent in steel building systems. This paper and the companion paper (Foley et al., 2008) simply summarize the observations made during the analyses conducted. One major item of note, however, is that better information regarding the catenary anchoring demands and capacities is needed. This information can serve as the basis for slab membrane strength computations and better estimates for the contribution of the composite steel-concrete floor deck system to the integrity of the building framing system. Finally, the capacity of steel studs as an anchoring mechanism should be assessed further.

ACKNOWLEDGMENTS

The authors would like to thank Thomas Schlafly of the American Institute of Steel Construction for his support and understanding in completing this work. The authors would also like to thank the AISC Committee on Research members for their input and comments as well as Kurt Gustafson of AISC for his very helpful recommendations. Special thanks are due to Brian Crowder of Naval Facilities Engineering Command–Atlantic and David Stevens of Protection Engineering Consultants. Their extraordinarily diligent review of the report on which this paper is based with subsequent detailed and insightful comments is greatly appreciated. The authors would also like to thank Professor Sherif El-Tawil of the University of Michigan for his review of the report on which the paper is based and recommended corrections in the literature review.

REFERENCES

ACI (1997), *ACI Design Handbook; SP-17(97)*, American Concrete Institute, Farmington Hills, MI.

ACI (2005), *Building Code Requirements for Structural Concrete (ACI 318-05) and Commentary (ACI 318R-05)*, American Concrete Institute, Farmington Hills, MI.

AISC (2001), *Load and Resistance Factor Design Manual of Steel Construction*, 3rd ed., American Institute of Steel Construction, Chicago, IL.

AISC (2005), *Specification for Structural Steel Buildings*, ANSI/AISC 360-05, American Institute of Steel Construction, Chicago, IL.

AISI (2001), *North American Specification for the Design of Cold-Form Steel Structural Members*, AISI/COS/NASPEC 2001, American Iron and Steel Institute, Washington, DC.

Allam, A., Burgess, I. and Plank, R. (2000), "Simple Investigations of Tensile Membrane Action in Composite Slabs in Fire," *International Conference on Steel Structures of the 2000's*, Istanbul, Turkey, pp. 327–332, www.shef.ac.uk/fire-research/publications.html.

Astaneh-Asl, A., Call, S.M. and McMullin, K.M. (1989a), "Design of Single Plate Shear Connections," *Engineering Journal*, AISC, Vol. 26, No. 1, pp. 21–31.

Astaneh-Asl, A., Liu, J. and McMullin, K.M. (2002), "Behavior and Design of Single Plate Shear Connections," *Journal of Constructional Steel Research*, Vol. 58, pp. 1121–1141.

Astaneh-Asl, A., Nader, M.N. and Malik, L. (1989b), "Cyclic Behavior of Double Angle Connections," *Journal of Structural Engineering*, ASCE, Vol. 115, No. 5, pp. 1101–1118.

Bailey, C.G., White, D.S. and Moore, D.B. (2000), "The Tensile Membrane Action of Unrestrained Composite Slabs Simulated Under Fire Conditions," *Engineering Structures*, Vol. 22, pp. 1583–1595.

Burgess, I.W., Huang, Z. and Plank, R.J. (2001), "Non-Linear Modeling of Steel and Composite Structures in Fire," *International Seminar on Steel Structures in Fire*, Shanghai, China, pp. 1–15, www.shef.ac.uk/fire-research/publications.html.

Cai, J., Burgess, I.W. and Plank, R.J. (2002), *A Generalized Steel/Reinforced Concrete Beam-Column Element Model for Fire Conditions*, University of Sheffield, Department of Civil and Structural Engineering, Sheffield, U.K., 40 p.

DeStefano, M. and Astaneh-Asl, A. (1991), "Axial Force-Displacement Behavior of Steel Double Angles," *Journal of Constructional Steel Research*, Vol. 20, pp. 161–181.

DeStefano, M., Astaneh-Asl, A., DeLuca, A. and Ho, I. (1991), "Behavior and Modeling of Double Angle Connections Subjected to Axial Loads," *1991 Annual Technical Session—Inelastic Behavior and Design of Frames*, Chicago, IL, Structural Stability Research Council, pp. 323–334,

DeStefano, M., DeLuca, A. and Astaneh-Asl, A. (1994), "Modeling of Cyclic Moment-Rotation Response of Double-Angle Connections," *Journal of Structural Engineering*, ASCE, Vol. 120, No. 1, pp. 212–229.

DOD (2005), *Unified Facilities Criteria (UFC)—Design of Buildings to Resist Progressive Collapse (UFC 4-023-03)*, www.wbdg.org/ccb/browse_cat.php?o=29&c=4.

FEMA (2000), *State of the Art Report on Connection Performance (FEMA-355D)*, SAC Joint Venture and Federal Emergency Management Agency, Washington, DC.

Foley, C.M., Martin, K. and Schneeman, C. (2007), *Robustness in Structural Steel Framing Systems,* Report No: MU-CEEN-SE-07-01, American Institute of Steel Construction, Chicago, IL, p. 253.

Foley, C.M., Schneeman, C.L. and Barnes, K.M. (2008), "Quantifying and Enhancing Robustness in Steel Structures: Part 1—Moment-Resisting Frames," *Engineering Journal*, AISC, Vol. 45, No. 4, pp. 247–266.

GSA (2003), *Progressive Collapse Analysis and Design Guidelines for New Federal Office Buildings and Major Modernization Projects,* www.oca.gsa.gov.

Hawkins, N.M. and Mitchell, D. (1979), "Progressive Collapse of Flat Plate Structures," *ACI Journal*, ACI, Vol. 76, No. 8, pp. 775–808.

Hibbeler, R.C. (2006), *Structural Analysis,* 6th ed., Pearson Prentice-Hall, Upper-Saddle River, NJ.

Huang, Z., Burgess, I.W. and Plank, R.J. (2000a), "Effective Stiffness Modelling of Composite Concrete Slabs in Fire," *Engineering Structures*, Vol. 22, pp. 1133–1144.

Huang, Z., Burgess, I.W. and Plank, R.J. (2000b), "Three-Dimensional Analysis of Composite Steel-Framed Buildings in Fire," *Journal of Structural Engineering*, ASCE, Vol. 126, No. 3, pp. 389–397.

Huang, Z., Burgess, I.W. and Plank, R.J. (2003a), "Modeling Membrane Action of Concrete Slabs in Composite Buildings in Fire. I: Theoretical Development," *Journal of Structural Engineering*, ASCE, Vol. 129, No. 8, pp. 1093–1102.

Huang, Z., Burgess, I.W. and Plank, R.J. (2003b), "Modeling Membrane Action of Concrete Slabs in Composite Buildings in Fire. II: Validations," *Journal of Structural Engineering*, ASCE, Vol. 129, No. 8, pp. 1103–1112.

Liu, J. and Astaneh-Asl, A. (2000a), "Cyclic Testing of Simple Connections Including Effects of Slab," *Journal of Structural Engineering*, ASCE, Vol. 126, No. 1, pp. 32–39.

Liu, J. and Astaneh-Asl, A. (2000b), *Cyclic Tests on Simple Connections Including the Effects of the Slab*, Report No. SAC/BD-00/03, SAC Joint Venture, p. 186.

Liu, R., Davison, B. and Tyas, A. (2005), "A Study of Progressive Collapse in Multi-Storey Steel Frames," *Proceedings of the 2005 Structures Congress and the 2005 Forensic Engineering Symposium*, New York, NY, American Society of Civil Engineers, CD-ROM.

Marchand, K.A. and Alfawakhiri, F. (2004), *Blast and Progressive Collapse*, Facts for Steel Buildings Number 2, American Institute of Steel Construction, Chicago, IL.

Mitchell, D. and Cook, W.D. (1984), "Preventing Progressive Collapse of Slab Structures," *Journal of Structural Engineering*, ASCE, Vol. 110, No. 7, pp. 1513–1532.

Owens, G.W. and Moore, D.B. (1992), "The Robustness of Simple Connections," *The Structural Engineer*, Vol. 70, No. 3, Institution of Structural Engineers, pp. 37–46.

Park, R. (1964), "Tensile Membrane Behaviour of Uniformly Loaded Rectangular Reinforced Concrete Slabs with Fully Restrained Edges," *Magazine of Concrete Research*, Vol. 16, No. 46, pp. 39–44.

Park, R., and Gamble, W.R. (1980), "Chapter 12—Membrane Action in Slabs," *Reinforced Concrete Slabs*, R. Park, ed., John Wiley & Sons, Inc., New York, NY, pp. 562–612.

Powell, G.P. (2005), "Progressive Collapse: Case Studies Using Nonlinear Analysis," *Proceedings of the 2005 Structures Congress and the 2005 Forensic Engineering Symposium*, New York, NY, American Society of Civil Engineers, CD-ROM.

Regan, P.E. (1975), "Catenary Action in Damaged Concrete Structures," *ACI Publication SP-48: Industrialization in Concrete Building Construction*, American Concrete Institute, Detroit, MI, pp. 191–224.

Rex, C.O. and Easterling, W.S. (2002), "Partially Restrained Composite Beam-Girder Connections," *Journal of Constructional Steel Research*, Vol. 58, pp. 1033–1060.

Shen, J. and Astaneh-Asl, A. (1999), "Hysteretic Behavior of Bolted-Angle Connections," *Journal of Constructional Steel Research*, Vol. 51, pp. 201–218.

Shen, J. and Astaneh-Asl, A. (2000), "Hysteresis Model of Bolted Angle Connections," *Journal of Constructional Steel Research*, Vol. 54, pp. 317–343.

Thornton, W.A. (1985), "Prying Action—A General Treatment," *Engineering Journal*, AISC, Vol. 22, No. 2, pp. 67–75.

Vulcraft (2005), *Vulcraft Steel Roof and Floor Deck Catalog*, Vulcraft—A Division of Nucor Corportation, www.vulcraft.com.

Wales, M.W. and Rossow, E.C. (1983), "Coupled Moment-Axial Force Behavior in Bolted Joints," *Journal of the Structural Division*, ASCE, Vol. 109, No. 5, pp. 1250–1266.

Wang, Y.C. and Kodur, V.K.R. (2000), "Research Toward Use of Unprotected Steel in Structures," *Journal of Structural Engineering*, ASCE, Vol. 126, No. 12, pp. 1442–1450.

Ziemian, R.D. and McGuire, W. (2000), *MASTAN2 Ver. 1.1*, John Wiley & Sons, New York, NY.